

## Strong intrinsic mixing in vortex magnetic fields

James E. Martin, Lauren Shea-Rohwer, and Kyle J. Solis  
 Sandia National Laboratories, Albuquerque, New Mexico 87185-1415, USA  
 (Received 7 March 2009; published 22 July 2009)

We report a method of magnetic mixing wherein a “vortex” magnetic field applied to a suspension of magnetic particles creates strong homogeneous mixing throughout the fluid volume. Experiments designed to elucidate the microscopic mechanism of mixing show that the torque is quadratic in the field, decreases with field frequency, and is optimized at a vortex field angle of  $\sim 55^\circ$ . Theory and simulations indicate that the field-induced formation of volatile particle chains is responsible for these phenomena. This technique has applications in microfluidic devices and is ideally suited to applications such as accelerating the binding of target biomolecules to biofunctionalized magnetic microbeads.

DOI: [10.1103/PhysRevE.80.016312](https://doi.org/10.1103/PhysRevE.80.016312)

PACS number(s): 47.51.+a, 47.57.-s, 47.61.Ne, 47.65.Cb

### I. INTRODUCTION

There are many cases where improved methods of fluid mixing are needed, especially in small confined geometries, such as microfluidic channels, where the low Reynolds numbers make it difficult to induce turbulence. There have been numerous attempts to address this problem with magnetic fields, and these fall into two classes: field gradient and uniform field techniques. Field gradients are used to generate forces on magnetic particles, and uniform fields are used to generate torques on acicular magnetic structures, or Lorentz forces on charges. The resulting fluid flow vastly accelerates mixing when compared to fluid diffusion times at the relevant length scales.

Methods relying on field gradients include shuttling particles through the fluid with a moving permanent magnet [1], spinning the fluid across permanent magnetic arrays [2], and flowing the fluid across wires that create a field gradient by current flow [3]. A strong roughly uniform dc magnetic field has been used to create a Lorentz force on ions transported between two electrodes [4], and a strong ac magnetic field has been used to rotate glass particles containing magnetite inclusions, apparently due to their small remanence [5].

Stir-bar strategies have been extended to the microscale by exposing either permanent or volatile acicular magnetic structures to a spatially uniform rotating magnetic field. Permanent structures include fabricated magnetic rods [6,7] and magnetite-loaded microbeads chemically bonded into chains [8]. These *extrinsic* methods produce a mixing torque that is limited by the low volume fraction of acicular structures that can be loaded into a fluid without serious congestion. A modest level of mixing can be achieved by exposing a fluid containing magnetite-loaded microbeads to a rotating field. At low volume fractions and field frequencies these beads will self-assemble into volatile chains, providing a modest level of mixing within the fluid [9,10]. When these beads are used to bind target biomolecules this mixing may be called *intrinsic*, since no foreign objects need be introduced to effect mixing. However, at higher field frequencies and particle loadings the time-average dipolar interaction between fixed spherical particles becomes negative, so particles form sheets, not chains, and mixing does not occur [11,12].

We have developed a different method of intrinsic magnetic mixing that generates large torques with modest fields.

Our approach is to apply a *vortex* magnetic field to a suspension of spherical magnetic particles. A vortex field is a rotating field created from two ac fields of identical frequency in quadrature phase, to which a third dc field component normal to the rotating field plane is added. The resulting field vector has the precessionlike motion illustrated in Fig. 1, and when the root-mean-square (rms) values of the three field components are equal we call the vortex field *balanced*.

To the first order, the time-average dipolar interaction between stationary particles vanishes in balanced triaxial fields [13], of which a balanced vortex field is a special case, so particles can only interact strongly when they form chains that follow the vortex field vector. The mixing torque is independent of particle size, so nanoscale volumes can be mixed with nanoparticles, and only the very modest fields that can be produced with Helmholtz coils are required. This method is effective with particles that do not have magnetic remanence, so it would be an ideal method of accelerating the binding of target biomolecules to functionalized “paramagnetic” microbeads, which would simultaneously provide the mixing torque.

The mixing effects created by a vortex field are striking. When 4–7  $\mu\text{m}$  iron particles are added to a low viscosity liquid they quickly settle. Subjecting this sediment to a 200

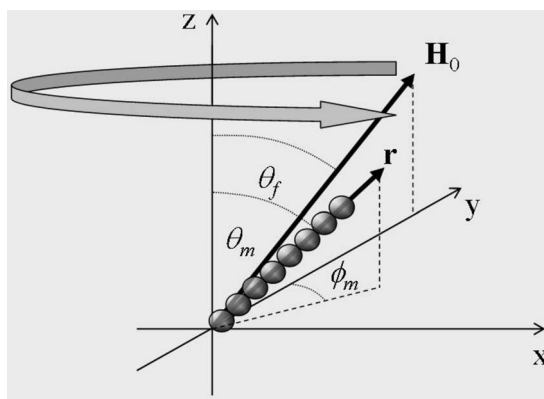


FIG. 1. The vortex field makes a constant angle  $\theta_f$  to the  $z$  axis, which is parallel to the dc field. The rotating field component is created by applying ac fields in quadrature phase along the  $x$  and  $y$  axes. A spherical particle chain makes an angle  $\theta_m$  with the  $z$  axis and exhibits an azimuthal phase lag  $\phi_m$ .

Hz rotating magnetic induction field produces no discernible effect until a dc magnetic field of comparable amplitude is applied normal to the rotating field plane. The sediment then disperses to form a suspension that whirls around in the sample cell. Increasing or decreasing the dc field greatly reduces this mixing. Vortex fields with amplitudes as modest as 0.02 T (200 G) rotate the fluid fast enough that the centrifugal force moves the opaque suspension up onto the walls of the cell, so that the cell bottom is free of fluid.

In this paper we report experiments designed to elucidate the microscopic mechanism of mixing, and these show some surprising effects. First, the mixing torque does not increase with field frequency. By contrast, a stir bar gives a mixing torque proportional to frequency until stagnation occurs. Second, the mixing torque is quadratic in the field, whereas with a stir bar the torque is field independent above the stagnation field. Third, with a soft magnetic material such as iron, the torque is nearly zero in a rotating field and maximizes when the dc component is comparable to the rotating field magnitude. Stir bars function optimally in a simple rotating field.

There are several factors that could give rise to a torque on a particle suspension in a vortex field. Each of these factors has a unique dependence on the strength of the vortex field, on the relative strength of the dc component of the vortex field, on the field frequency, and on the fluid viscosity.

Particle *shape anisotropy* will cause a soft magnetic particle to preferentially align with its long axis parallel to the instantaneous magnetic field. In a vortex field an acicular particle will have a precessionlike motion that will impart torque to the fluid. Above the stagnation field this mixing torque will be independent of the field, since the particle will rotate at the field frequency. The torque will be optimal in a simple rotating field, because this maximizes the moment of the particle around the mixing axis, and will increase in proportion to field frequency until stagnation occurs. Finally, the torque will increase with fluid viscosity until stagnation occurs and, thus, will vanish for particles in a solid matrix. An analysis of a nanorod in a vortex field explores these issues [14], and a more recent paper on isolated ellipsoidal particles explores some of these issues as well, including the residual asynchronous motion that occurs in the stagnation regime [15].

A *frequency-dependent susceptibility* will cause the dipole moment of a particle to lag behind the field, creating torque. This torque will increase with frequency, reach a maximum, and then decrease. This torque will be insensitive to fluid viscosity and will persist even for particles in a solid matrix. The torque will be strong in a rotating field.

Particle *agglomerates* can lead to a fluid torque if the agglomerates have a susceptibility anisotropy. For example, a low-frequency rotating field applied to a very dilute suspension will assemble particles into chains. Magnetic measurements on particle chains show that the susceptibility parallel to a chain is nearly three times larger than perpendicular. Because of this, a chain will rotate with the applied field. However, a chain is not a simple stir bar; it is a volatile structure that can grow through aggregation or shrink through fragmentation induced by hydrodynamic forces. A full consideration of particle chaining in a vortex

magnetic field is involved [14], but the results are easily summarized. The torque will increase with the field energy density, will be roughly independent of the field frequency, and will vanish for a solid composite. Finally, the application of a dc field is essential to torque production. If the dc field is too small the agglomerates will have a sheetlike structure with a negligible susceptibility anisotropy; if the dc field is too large, the chains will tend to grow without bound and collapse along the vertical (mixing) axis, producing negligible torque.

## II. EXPERIMENT

Torque measurements were made on 4–7  $\mu\text{m}$  carbonyl Fe powders obtained from Lord Corporation, chosen for their low remanence. These particles were either dispersed in liquids of differing viscosities  $\eta$  [ethanol, with  $\eta=1$  cP at 25 °C, benzyl alcohol (8 cP) or ethylene glycol (16 cP)] or immobilized by a polymerizable resin to create a solid composite. Typically, 150 mg of Fe particles were dispersed in 2 ml liquid to create a 1.0 vol. % suspension.

Torques were measured by suspending the samples into the triaxial magnet with a 0.75-mm-diameter nylon torsion fiber and measuring the angular displacement of the vial in the field. The vortex field has three parameters: frequency  $f$ , magnitude  $H_0$ , and polar field angle  $\theta_f$ . These parameters are defined through

$$\mathbf{H}_0 = H_0 \{ \sin \theta_f [ \sin(2\pi ft) \hat{x} + \cos(2\pi ft) \hat{y} ] + \cos \theta_f \hat{z} \},$$

so the dc field (mixing axis) is in the  $z$  direction. For a balanced vortex field the three rms field components are equal, so  $\sin \theta_f = \sqrt{2/3}$ ,  $\cos \theta_f = \sqrt{1/3}$ , and  $\theta_f \approx 54.7^\circ$ .

## III. RESULTS

We first examine the dependence of the mixing torque on the magnitude of a *balanced* vortex field, comprised of a rotating field and a vertical field whose magnitude is equal to the rms value of either of the rotating field components. The vortex angle of such a field is  $\text{atan}(\sqrt{2}) \approx 54.7^\circ$ , the so-called magic angle in NMR. Measurements on an ethanol suspension show a nearly field-squared dependence, Fig. 2(a), over the frequency range of 100–500 Hz, but the more viscous ethylene glycol suspensions show a complex field dependence, Fig. 2(b), especially at 500 Hz, where the torque is low at low fields. These measurements indicate that particle agglomerates, probably chains, produce mixing. The vortex field produces little torque on the solidified suspension, so the frequency-dependent susceptibility of Fe plays a negligible role.

The second issue is the dependence of the torque on the vortex field angle  $\theta_f$ . The results in Fig. 3 show a maximum torque at a vortex field angle near  $60^\circ$ —essentially a balanced vortex field. The torque falls off rapidly at higher angles because the particles form sheetlike structures [12] that have negligible susceptibility anisotropy in the plane. The falloff at lower angles is discussed below.

The ethylene glycol data in Fig. 4(a) show that the mixing torque is essentially independent of frequency at the highest

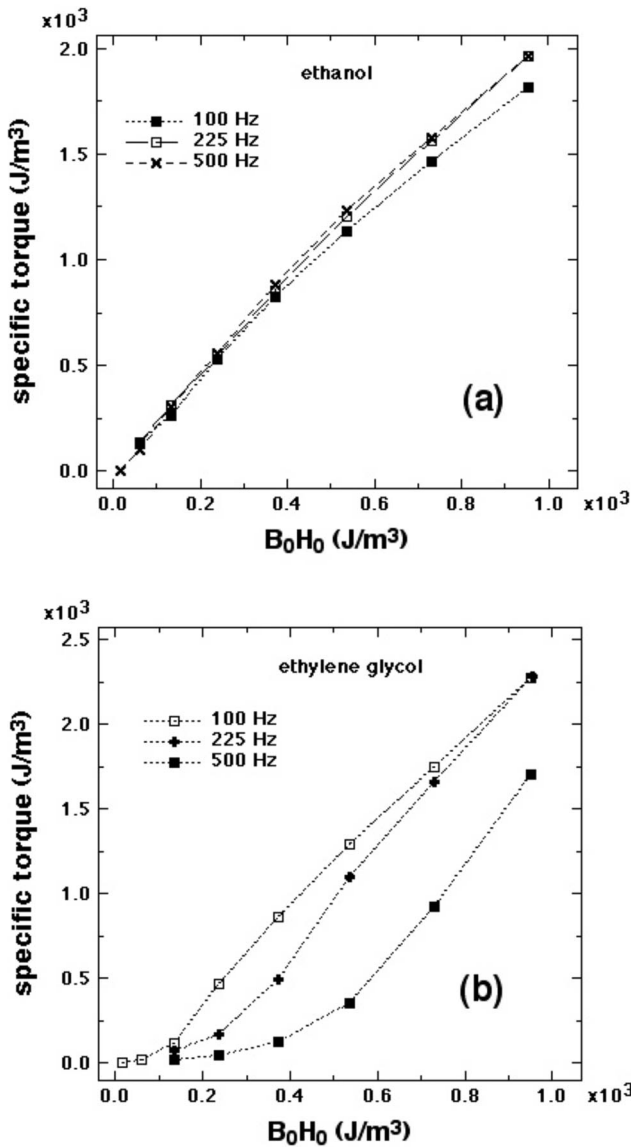


FIG. 2. The specific torque density (torque per unit volume of particles) of Fe particles in balanced vortex fields ( $\theta_f \approx 54.7^\circ$ ) is shown as a function of field strength. (a) The specific torque density in ethanol is essentially independent of field frequency and roughly quadratic in the field, although at higher fields the effect of magnetic saturation is apparent. (b) In ethylene glycol, which has a viscosity 16 times that of ethanol, the field dependence is much more complex, especially at 500 Hz, where mixing is very weak at low fields.

field strength and falls off rapidly with frequency at the lowest. Furthermore, Fig. 4(b) shows that at 500 Hz the torque decreases with increasing viscosity. These trends are opposite to that expected for fluid mixing by particle rotation, which should be quite similar to mixing with a magnetic stir bar, and we shall see that this is a complex aspect of torque production by volatile agglomerates.

IV. DISCUSSION

The experimental results we have shown can be explained by the field-induced formation of particle chains, the shape

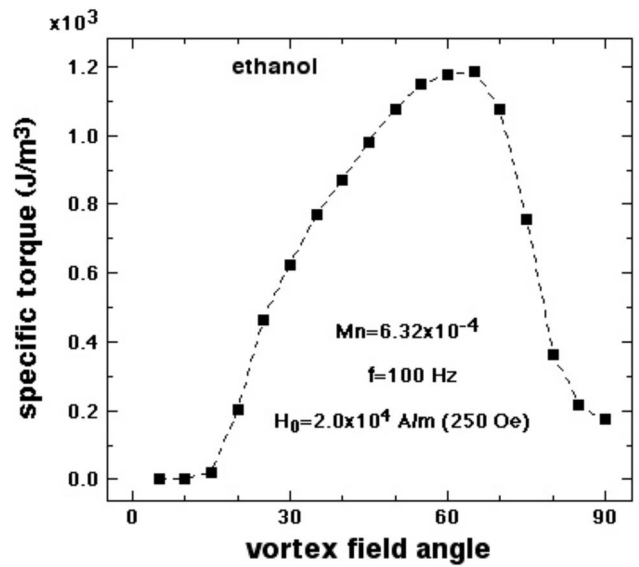


FIG. 3. The specific torque density of Fe particles in ethanol is strongly dependent on the vortex field angle, with a maximum near a balanced vortex field.

of which is shown in the dynamical simulation in Fig. 5. As shown in Fig. 1, these chains follow the vortex field, but with a phase lag  $\phi_m$  in the azimuthal angle swept out by the field. This phase lag decreases with field strength and increases with chain length, field frequency, and fluid viscosity. As the phase lag increases, the polar angle of the chain to the dc field  $\theta_m$  decreases. This reduces the moment of the chain and thus the mixing torque.

Particle chains are volatile structures that are held together by the magnetic interactions between particles, which must be strong enough to balance the viscous forces on the spinning chains. Larger fields promote the formation of longer chains, and higher frequencies reduce the average chain length. In general, spinning chains will aggregate to form longer chains until the viscous forces dominate the magnetic forces, at which point a chain will fragment near its center. The physical picture is similar to the chain model of electro-rheology and magneto-rheology [16], but the geometry is more complex.

An analysis of chains in a vortex field [14] leads to results that are consistent with our experimental observations. First, the torque density in the fluid is given by

$$T = \frac{1}{12} \phi_p \mu_o M^2 \sqrt{\sin^2 \theta_f - \cos^2 \theta_f} \quad \text{for } \theta_f \geq 45^\circ, \quad (1)$$

where  $\phi_p$  is the particle volume fraction,  $M$  is the particle magnetization, and  $\mu_o$  is the vacuum permeability. This expression predicts that the mixing torque is proportional to the field squared at low fields and is independent of field frequency, fluid viscosity, and most notably, particle size. Our data show these effects, as well as more complex behavior that arises when the experimental conditions do not strongly support mixing (i.e., low field, high frequency, high viscosity).

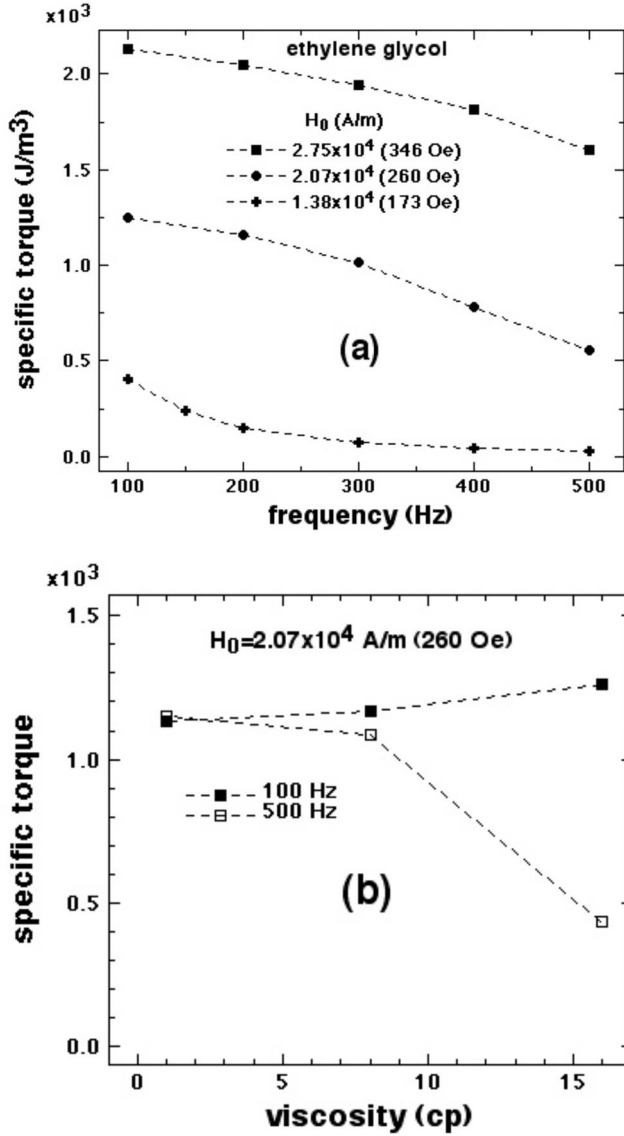


FIG. 4. The specific torque density of Fe particles in balanced vortex fields ( $\theta_f \approx 54.7^\circ$ ) is shown as a function of frequency and viscosity. (a) At the highest field the torque is essentially independent of frequency, but at the lowest field it decreases rapidly with frequency. (b) The torque density is independent of liquid viscosity at 100 Hz but decreases with viscosity at 500 Hz.

The transition from mixing to quiescent regimes is governed by the so-called Mason number  $Mn$ , a ratio of the viscous forces that tend to fragment particle agglomerates to the magnetic forces that cause agglomeration. In terms of the liquid viscosity  $\eta$  and the field frequency  $\omega$ ,

$$Mn = \frac{9}{2} \frac{\eta \omega}{\mu_0 M^2}. \quad (2)$$

Our expression for the mixing torque is only valid for very small  $Mn$ , where the dominant magnetic interactions promote particle chaining. A calculation shows that the maximum stable chain size is related to the Mason number through

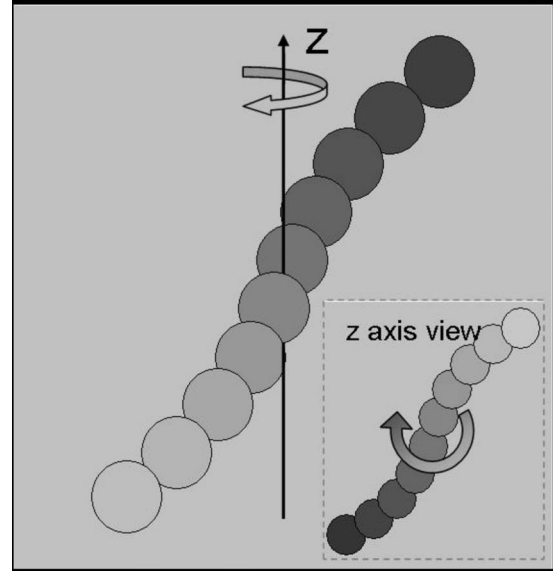


FIG. 5. Brownian dynamics simulation of a chain in a balanced vortex field shows the curvature of a chain near its maximum possible length. Inset is the view along the mixing axis.

$$N_{\max}^2 = \frac{1}{16Mn\sqrt{\sin^2 \theta_f - \cos^2 \theta_f}} \quad \text{for } \theta_f \geq 45^\circ, \quad (3)$$

where the number of particles in a chain is  $2N$ . The maximum chain size increases with the field, decreases with increasing viscosity and field frequency, and is independent of the particle size. Remarkably, the change in the chain size with these parameters is exactly what is needed to keep the mixing torque constant. This strange behavior is a manifestation of the well-known shear-thinning viscosity of magneto-rheological fluids in an applied field.

The transition from the mixing to quiescent regimes is due to the failure of chain formation. Above a *critical Mason number*  $Mn^*$  the viscous forces so dominate the magnetic forces that even particle dimers do not form. By substituting  $N_{\max} = 1$  into Eq. (3) this *critical Mason number* is shown to be

$$Mn^* = \frac{1}{16\sqrt{\sin^2 \theta_f - \cos^2 \theta_f}} \quad \text{for } \theta_f \geq 45^\circ. \quad (4)$$

In a balanced vortex field particles chain only when the Mason number is smaller than roughly 0.1.

Although we cannot predict how the mixing torque will falloff when the Mason number exceeds  $Mn^*$ , we can still use the Mason number to create a master curve that demonstrates that particle agglomeration is responsible for mixing. To compute the Mason number at low fields we use  $M = \chi_p H_0$  for the particle magnetization and the theoretical value  $\chi_p = 3$  for the *apparent* susceptibility of a sphere of high susceptibility magnetic material such as iron [17]. The torque density should then be of the form  $T = \frac{\sqrt{3}}{4} \phi_p B_0 H_0 g(Mn)$ , where  $g(Mn) = 1$  for  $Mn \ll Mn^*$  and is monotonically decreasing for  $Mn \gg Mn^*$ . Data plotted on the dimensionless axes  $T/(\phi_p B_0 H_0)$  versus  $Mn$  should thus yield

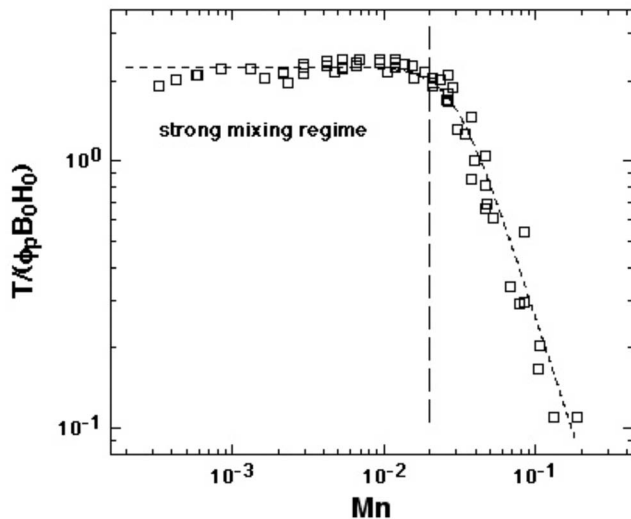


FIG. 6. Plotting all of the balanced vortex field data in Figs. 2(a), 2(b), 4(a), and 4(b) on dimensionless axes suggested by the chain model results in a master curve that affirms the conclusion that particle agglomeration is responsible for mixing. Strong mixing, described by Eq. (1) and indicative of robust chaining, is observed for  $Mn < 0.02$ . Mixing is essentially nonexistent (90% lower) above the critical Mason number of 0.1.

a master curve. Plotting the data in Figs. 2(a), 2(b), and 4 on these axes yields the master curve in Fig. 6. The chain model thus predicts the mixing behavior in the strong mixing regime, where  $Mn < 0.02$ . Above the predicted critical Mason number of 0.1 the torque should technically be zero, and it is indeed 90% smaller than in the strong mixing regime. The maximum amplitude of  $\sim 2$  of the dimensionless torque  $T / (\phi_p B_0 H_0)$  is more than four times our predicted value of  $\sqrt{3}/4 \approx 0.43$ . In fact, accounting for local dipolar fields increases the predicted dimensionless torque amplitude to 1.0 (see Eq. 34 of Ref. [14]), and the remaining factor-of-2 discrepancy can be partly attributed to the fact that the particles are somewhat aspherical, which increases their magnetization in a given applied field [17]. But an additional source of this discrepancy is that the chain model we have proposed only accounts for dipolar interactions, which is only correct in saturating magnetic fields. For multidomain particles in low fields multipolar interactions significantly increase the interaction force [16].

The dependence of the measured torque on vortex field angle is not easily explained. Equation (1) predicts that the

torque should vanish for vortex field angles smaller than  $45^\circ$ , a trend seen in the experimental data. This falloff occurs because for low vortex angles it is possible for particle chains to grow without limit and align with the dc field, becoming stationary. For vortex field angles larger than  $45^\circ$  this alignment cannot occur because the chains become unstable and fragment as their phase lag increases and their polar angle decreases. For large vortex angles Eq. (1) does not apply because the particles form stationary sheets, not chains, under such circumstances [13]. In fact, vortex mixing works better than predicted at smaller vortex angles, and we attribute this to the fact that the shear field in the fluid itself causes the chains to fragment at lower field angles. The *single chain model* we have proposed assumes that this fluid is stationary, in other words, we have ignored the collective hydrodynamic interactions of a many-chain system.

The second reason a balanced vortex field is so effective for mixing is that it does not strongly favor the formation of competing stationary structures. This is because in a balanced field the negative dipolar interaction produced by the rotating field on a pair of *stationary* particles cancels, to the first order, the positive dipolar interaction produced by the dc field [13]. In fact, the formation of stationary structures is possible, but only for Mason numbers exceeding  $Mn^*$ .

## V. CONCLUSIONS

We have shown that magnetic particle suspensions can be efficiently mixed in a balanced vortex field. This mixing is much more effective than that produced by a simple rotating field and is due to the formation of volatile particle chains that follow the field with a precessionlike motion. In the low Mason number, chain-forming regime, the mixing torque increases quadratically with the field and is independent of the field frequency, fluid viscosity, and particle size. This mixing technique is a viable technology for mixing problems on any scale, including mixing in microchannels and accelerating the binding of biomolecules to surface-functionalized magnetite-loaded microbeads.

## ACKNOWLEDGMENTS

Sandia is a multiprogram laboratory operated by Sandia Corporation, a Lockheed Martin Company, for the United States Department of Energy under Contract No. DE-AC04-94AL85000. This work was supported by the Division of Materials Science, Office of Basic Energy Sciences, U.S. Department of Energy (DOE).

[1] M. Herrmann, T. Veres, and M. Tabrizan, *Lab Chip* **6**, 555 (2006).  
 [2] M. Grumann, A. Geipel, L. Riegger, R. Zengerle, and J. Duce, *Lab Chip* **5**, 560 (2005).  
 [3] H. Suzuki, N. Kasagi, and C.-M. Ho, Proceedings of the 3rd International Symposium on Turbulence and Shear Flow Phenomena, Sendai Japan, 2003, pp. 817–822 (unpublished).

[4] H. H. Bau, J. Zhong, and M. Yi, *Sens. Actuators B* **79**, 207 (2001).  
 [5] A. Rida and M. A. M. Gijs, *Anal. Chem.* **76**, 6239 (2004).  
 [6] L.-H. Lu, K. S. Ryu, and C. Liu, *J. Microelectromech. Syst.* **11**, 462 (2002).  
 [7] P. K. Yuen, G. Li, Y. Bao, and U. R. Muller, *Lab Chip* **3**, 46 (2003).

- [8] S. L. Biswal and A. P. Gast, *Anal. Chem.* **76**, 6448 (2004).
- [9] S. Melle, G. G. Fuller, and M. A. Rubio, *Phys. Rev. E* **61**, 4111 (2000).
- [10] S. Melle and J. E. Martin, *J. Chem. Phys.* **118**, 9875 (2003).
- [11] T. C. Halsey, R. A. Anderson, and J. E. Martin, *Int. J. Mod. Phys. B* **10**, 3019 (1996).
- [12] J. E. Martin, R. A. Anderson, and C. P. Tigges, *J. Chem. Phys.* **108**, 7887 (1998).
- [13] J. E. Martin, R. A. Anderson, and R. L. Williamson, *J. Chem. Phys.* **118**, 1557 (2003).
- [14] J. E. Martin, *Phys. Rev. E* **79**, 011503 (2009).
- [15] P. Tierno, J. Claret, F. Sagues, and A. Cebers, *Phys. Rev. E* **79**, 021501 (2009).
- [16] J. E. Martin and R. A. Anderson, *J. Chem. Phys.* **104**, 4814 (1996).
- [17] J. A. Osborn, *Phys. Rev.* **67**, 351 (1945).